J Electroceram (2008) 20:225–229
DOI 10.1007/s10832-007-9181-8

Application of Ag–ceramic composite electrodes to low firing piezoelectric multilayer ceramic actuators

Mun-Seok Choi · Sung-Hoon Kim · Young-Hyeok Kim · Ill Won Kim · Soon-Jong Jeong · Jae-Sung Song · Jae-Shin Lee

Received: 13 November 2006 / Accepted: 20 June 2007 / Published online: 2 August 2007

Abstract Ag–ceramic composite materials were investigated as low-cost internal electrodes for low firing piezoelectric multilayer ceramic actuators (MLCA). Ag–ceramic pastes were prepared by adding $Pb(Mg_{1/3}Nb_{2/3})O_3$–$Pb(Zr_{0.475},Ti_{0.525})O_3$ (PMNZT) ceramic powders to a commercial Ag paste in the range of 0 to 50 wt.%. PMNZT/Ag–PMNZT multilayered laminates were fabricated using tape casting and subsequently cofired at 925°C for 10 h. The addition of PMNZT into Ag electrode decreased the thermal shrinkage mismatch between the composite layers, which led to improve mass producibility of MLCA through reducing delamination probability during cofiring process.

Keywords Piezoelectric ceramics · Multilayer actuator · Internal electrode · Low firing

1 Introduction

Piezoelectric and electrostrictive materials for actuators are widely used in applications requiring precision displacement control or high generative force, i.e. optical stage, precision mechatronics, and semiconductor devices [1, 2]. In particular, multilayer ceramic actuators(hereafter, MLCA) have been extensively explored because their assets are a rapid operation, a low power consumption, a high precision control and little noise [3, 4], compared with conventional electromagnetic actuators. However, the reliability of MLCA has been of main concern because of process induced defects and their propagation caused by fatigue phenomena during service.

It is generally considered that delamination between the internal electrode and the ceramic and/or microcracks at the interface during processing would act as nuclei for crack propagation. The delamination is mainly due to inadequate adhesion of the internal electrode and piezoelectric ceramic layer, catalytic reaction of electrode metals with organic additives during burnout and cofiring densification mismatch [5, 6]. Also, the mismatch of thermal contraction properties easily leads to the development of microcracks at the interfaces or internal stresses during cooling and soldering. Generally speaking, these microcracks and interfacial defects are mainly responsible for the fatigue and degradation of MLCA [7, 8].

Currently most MLCA adopt expensive AgPd alloys as internal electrodes because they are stable between piezoelectric ceramic layers throughout high temperature sintering process. Therefore there is ample necessity to explore inexpensive conducting materials as an internal electrode for low cost and low firing MLCA [9]. Low temperature sintering has been attempted using a wide variety of methods: sol–gel method [10], hot-pressing in oxygen [11], fine powders prepared by high energy ball-milling [12], and low melting sintering aids such as $LiBiO_2$, Li_2CO_3, and so on [13, 14]. Ternary $Pb(Mg_{1/3}Nb_{2/3})O_3$–$Pb(Zr,Ti)O_3$ (abbreviated as PMNZT) ceramics exhibit high piezoelectric constants near the morphotropic phase boundary. Our previous researches demonstrated that Li_2O added PMNZT ceramics show good

M.-S. Choi · S.-H. Kim · Y.-H. Kim · J.-S. Lee (✉)
School of Materials Science and Engineering, University of Ulsan, P.O. Box 18, Nam-Ulsan 680-749, South Korea
e-mail: jslee@uou2.ulsan.ac.kr

I. W. Kim
Department of Physics, University of Ulsan, Nam-Ulsan, South Korea

S.-J. Jeong · J.-S. Song
Electric and Magnetic Devices Group, KERI, Changwon, South Korea

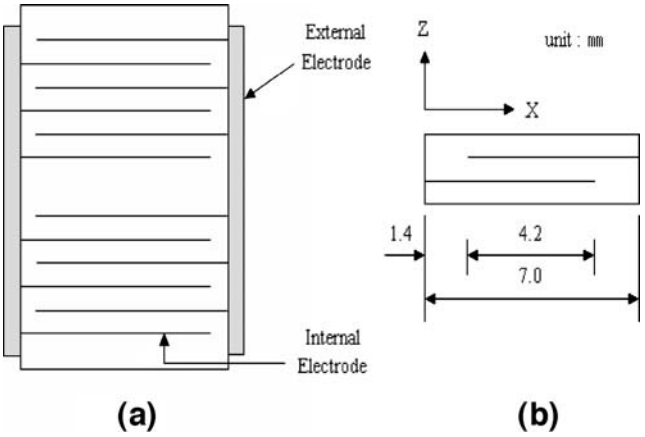

Fig. 1 (**a**) Cross-section and (**b**) dimension of MLCA

piezoelectric characteristics after firing at temperature as low as 950°C [15], which is lower than the melting point of Ag (961°C). In the present study, we investigated Ag–PMNZT ceramic composite materials as internal electrodes for low firing piezoelectric multilayer actuators. This paper reports the electrical and thermal properties of Ag–PMNZT composites as well as the piezoelectric properties of PMNZT/Ag–PMNZT multilayer actuators.

2 Experiments

Ceramic powders with a composition of $0.2Pb(Mg_{1/3}Nb_{2/3})O_3$–$0.8Pb(Zr_{0.475},Ti_{0.525})O_3$ were synthesized using the columbite precursor method that consists of two-stage calcination processes. In the first step, a mixture of MgO, Nb_2O_5, ZrO_2 and TiO_2 powders were properly weighed and ball-milled with zirconia balls and deionized water for 24 h. The mixed powders were dried and then calcined at 1100°C for 4 h to form a columbite phase of $MgNb_2(Zr,Ti)O_6$. In the second step, a stoichiometric amount of PbO was added and mixed with calcined powders by ball-milling for 24 h again. After drying, it was re-calcined at 900°C for 2 h. Before milling the calcined powders, 0.1 wt.% Li_2CO_3 was added as a sintering aid.

Ag–ceramic composite pastes were prepared by mixing the PMNZT powders in a commercially available Ag electrode paste (SJA-73-731, Sung Jee Tech, Korea) with a solid content of 85 vol.%. In this study, the concentration of PMNZT powder in the composite paste was varied from 0 to 50 wt.%. For microstructure analysis, Ag–ceramic pellets were also prepared using conventional dry pressing after drying solvents in a oven.

PMNZT/Ag–PMNZT MLCA with a configuration shown in Fig. 1 were fabricated in this work. Piezoelectric ceramic sheets were obtained by tape casting ceramic slurry containing a mixture of PMNZT powders, organic binders, a plasticizer and solvents. The green sheets were cut into 10×10 cm^2 using a knife cutting machine. The Ag–ceramic paste was screen-printed on the ceramic sheet, and then laminated with 40-layers of PMNZT sheets. After soaking at 500°C for 6 h in air for removing the organic additives contained in the green sheets, the laminated composites were cofired at 925°C for 10 h in air.

The microstructure and crystal structure of Ag–ceramic were observed using an optical microscope equipped with an image analyzer (Olympus PMG3, Japan) and an X-ray diffractometer (Rigaku RAD-3C, Japan). The electrical conductivity of Ag–ceramic composites was characterized using four-point probe method after screen printing Ag–ceramic paste on an alumina plate and subsequent sintering at 925°C for 2 h. The thermal shrinkage of Ag–ceramic composites was characterized with a computer controlled thermomechanical analyzer (Shimadzu TMA-50, Japan). The electric field induced actuation characteristics of MLCA were examined with a laser displacement measurement system (Demodulator-3700, GRAPHTEC, Japan).

3 Results and discussion

3.1 Physical properties of Ag–PMNZT composite electrodes

Crystal structures of Ag–PMNZT composites were observed after sintering pellet specimens at 925°C for 2 h in air. Figure 2 represents XRD patterns of Ag–ceramic composites for different ceramic concentrations. The phases were identified as the face centered cubic Ag [17] and the

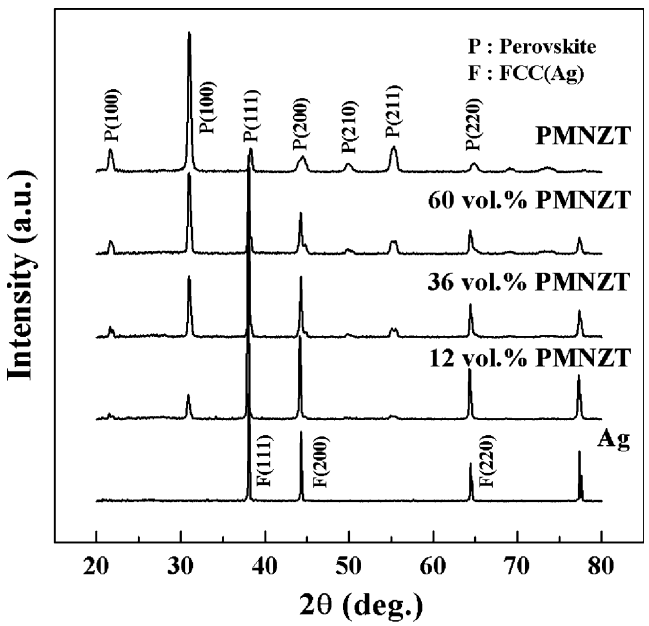

Fig. 2 X-ray diffraction patterns of sintered Ag–PMNZT composites as a function of the ceramic concentration

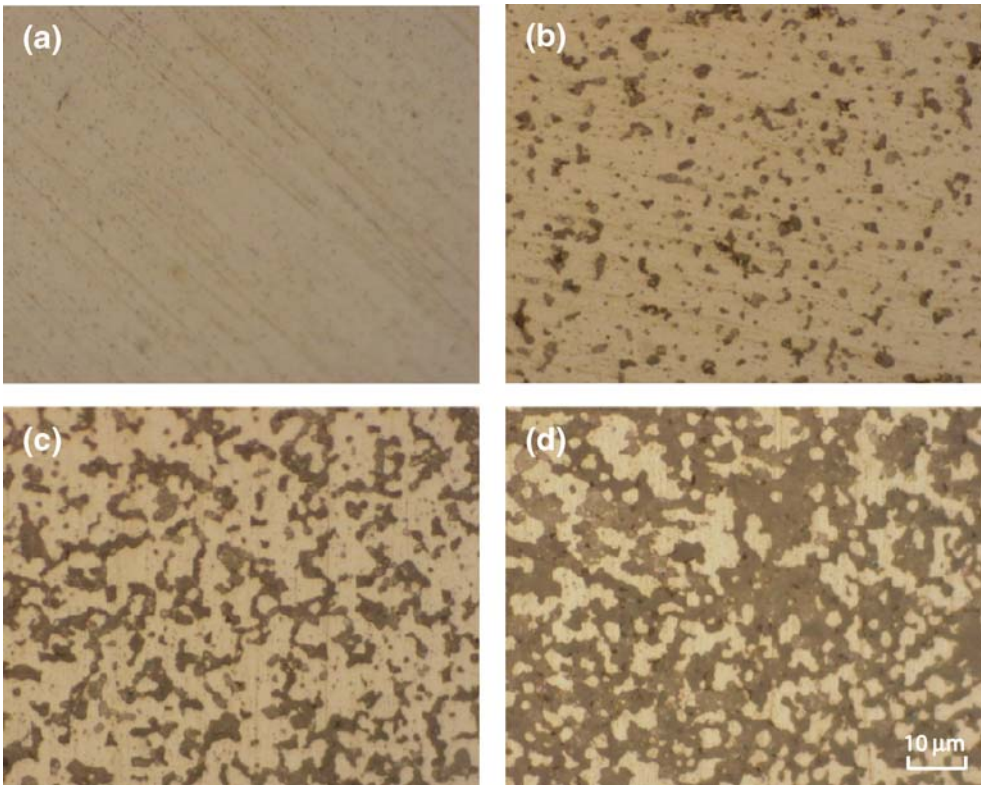

Fig. 3 Polished surface micrographs of sintered Ag–PMNZT composites for different ceramic concentrations. The PMNZT powder concentrations in Ag paste were (**a**) 0, (**b**) 10 wt.%, (**c**) 30 wt.%, and (**d**) 50 wt.%, respectively

rhombohedral perovskite phase [18], respectively. This indicates that the chemical reaction between Ag and PZT at the firing temperature is insignificant, and thus Ag can be effectively applied to the internal electrodes of MLCA using PMNZT piezoelectric ceramics. Kondo et al. [9] also reported that Ag was cofirable with $Pb(Ni_{1/3}Nb_{2/3})O_3$–$Pb(Zr,Ti)O_3$ ceramics at 900°C for MLCA fabrication.

Figure 3 shows the micrographs of polished surface of Ag–ceramic composites fired at 925°C for 2 h in air. Two phases identified with XRD analysis, as given in Fig. 1, are clearly seen in the micrographs as bright Ag and dark PMNZT phases, respectively. With elevating the concentration of PMNZT ceramics, the area fraction of dark phase increases. The area fractions of PMNZT in the composites

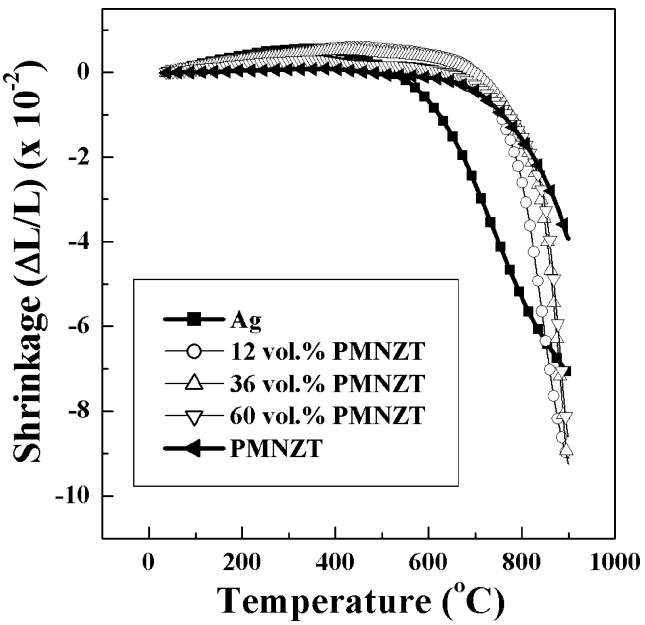

Fig. 4 Thermal shrinkage curves of Ag-PMNZT powder compacts

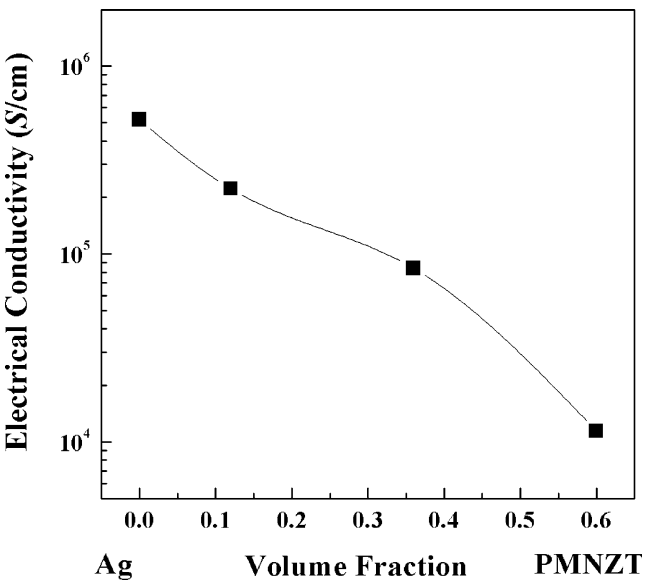

Fig. 5 Effects of ceramic content on electrical conductivity of Ag-PMNZT ceramic composites

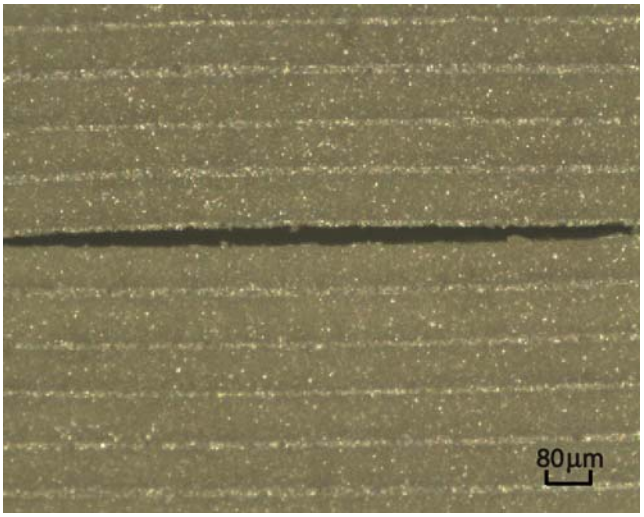

Fig. 6 Typical defects observed in PMNZT/Ag-PMNZT multilayer composites after sintering

characterized with an image analyzer were 0.12, 0.36 and 0.60 for 10, 30, and 50 wt.% ceramic added specimens, respectively. Because the area faction in the cross-section of a specimen matches to the volume fraction, the following relation can be derived;

$$f_v = 0.12 f_w$$

where f_v and f_w are the volume fraction in a sintered composite and the weight fraction of PMNZT phase in a composite paste with solvents, respectively.

A mismatch in the thermal contraction between different materials can cause significant defects of multilayered composites during sintering process. Figure 4 shows the thermal shrinkage curves of Ag–ceramic powder compacts as a function of the ceramic concentration. Pure Ag powders start to shrink at about 500°C, whilst the piezoelectric PMNZT ceramics do at higher temperature of 700°C. It is seen that the mismatch in the thermal shrinkage between Ag and PMNZT at temperatures of 500~900°C can be greatly reduced by adding PMNZT powders into Ag paste.

Table 1 Effects of PMNZT ceramic powder contents in the internal electrode on the firing failure rate of PMNZT/Ag–PMNZT multilayer composites.

Parameters	Values			
Ceramic volume fraction	0	0.12	0.36	0.60
Failure rate (%)	51.0	12.2	20.4	53.1

Figure 5 shows the effects of ceramic content on the electrical conductivity of Ag–ceramic composite thick films sintered at 925°C for 2 h. The measured electrical conductivity of the Ag thick film, 5.2×10^5 S/cm, is slightly lower than that reported in the literature for pure Ag, 6.8×10^5 S/cm [16]. This is probably due to the insulating glass frits contained in the thick film paste, which is generally added to enhance the adhesion strength between the thick film and the substrate. The conductivity falls down with the PMNZT ceramic concentration as indicated on the figure. It is interesting that the conductive characteristic of the composite is still maintained at as high ceramic concentration as 60 vol.% despite that the Ag phase looks isolated by insulating PMNZT ceramics, as seen in Fig. 3(d).

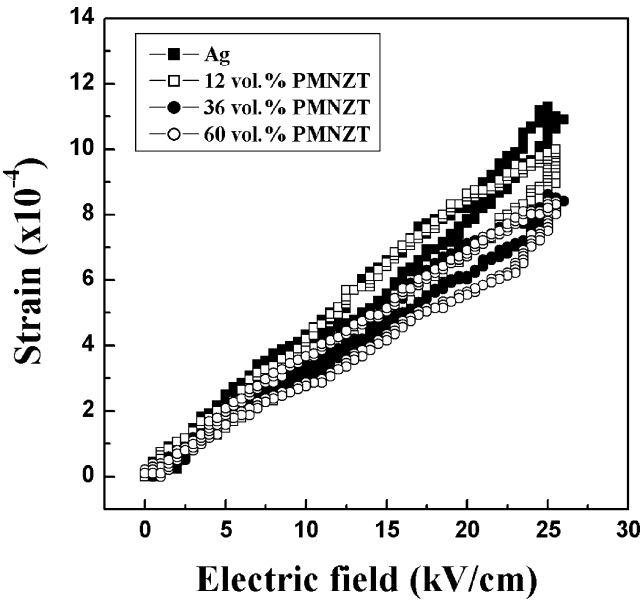

Fig. 7 Electric field induced strain of MLCA for different electrode compositions

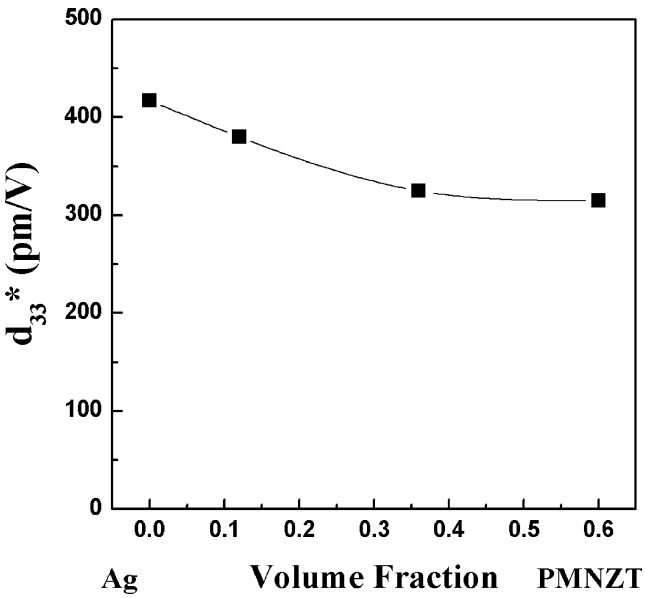

Fig. 8 The apparent piezoelectric coefficient (d_{33}*) of PMNZT/Ag-PMNZT multilayer composites as a function of the electrode composition

3.2 Properties of PMNZT/Ag–PMNZT multilayer actuators

Multilayer structures of piezoelectric ceramic sheet and internal electrodes were fabricated by laminating ceramic green sheets with screen-printed Ag–ceramic electrode. After the following cofiring step many specimens revealed delamination phenomena. A typical defect observed in the multilayer structure is shown in Fig. 6. The crack was mostly formed along the interfaces between the electrode and ceramic layers, strongly suggesting that the thermal shrinkage mismatch between two different layers is mainly responsible for such failure.

The failure rate in the cofiring step was explored by careful observation of a batch of specimens that were put on a saggar in a 7×7 array during firing process. The number of cracked specimens after firing was statistically counted among 49 specimens for four batches with different electrode compositions and the results are summarized in Table 1. In case of MLCA using pure Ag as internal electrodes, the failure rate was as high as 51% due to the large mismatch in the thermal shrinkage between composite layers during firing as represented in Fig. 4. However, the addition of 12 vol.% PMNZT ceramics into the Ag electrode drastically reduced the failure rate down to 12.2% because of the reduced shrinkage mismatch between layers. Although the reasons are not clear so far, the increased failure rate for specimens with higher ceramic concentrations in the electrode might be attributed to the lower adhesion strength between layers at the lamination step.

Figure 7 shows the microactuation characteristics of PMNZT/PMNZT–Ag multilayer actuators. The thickness of PMNZT ceramic layer and the number of stacked layers were about 80 and 40 μm, respectively. Apparent piezoelectric coefficients (d_{33}*) were calculated from the ratio of the maximum strain to the maximum filed on the curves, and replotted in Fig. 8. In case of MLCA using pure Ag as internal electrodes, the d_{33}* was calculated as 416 pm/V and well matched to the low-filed piezoelectric coefficient (d_{33}) of 412 pC/N that was measured for a bulk specimen with a Berlincourt d_{33} meter. With raising the ceramic content in the electrode, the apparent piezoelectric constant d_{33}* decreases due to the reduced area fraction of conducting Ag in the composite electrode as shown in Fig. 3.

4 Conclusions

Ag–PMNZT composite conductors were successfully applied to internal electrodes of low firing multilayer ceramic actuators. The addition of piezoelectric ceramic powders into Ag paste markedly reduced the thermal shrinkage mismatch between ceramic/electrode multilayer composites, while the effective electrode area and its electrical conductivity decreased with the ceramic concentration. The reduced mismatch in the thermal shrinkage between composite layers greatly improved the mass producibility in MLCA fabrication.

Acknowledgements This research was supported by a grant from Center for Advanced Materials Processing of 21st Century Frontier R & D Program funded by the Ministry of Commerce, Industry and Energy (MOCIE), Republic of Korea. Also this work was partly supported by the Ministry of Education and Human Resources Development (MOE), the MOCIE and the Ministry of Labor (MOLAB) through the fostering project of the Lab of Excellency.

References

1. Y. Yee, H.J. Nam, S.H. Lee, J.U. Bu, J.W. Lee, Sens. Actuators **89**, 166 (2001)
2. S. Wang, J.F. Li, K. Wakabayashi, M. Esashi, R. Watanabe, Adv. Mater. **10**, 874 (1999)
3. S. Takahashi, Jpn. J. Appl. Phys. **24**(Suppl. 24-2), 41 (1985)
4. M. Suga, M. Tsuzuki, Jpn. J. Appl. Phys. **23**(6), 765 (1984)
5. R. Zuo, L. Li, X. Hu, Z. Gui, Mater. Lett. **51**, 504 (2001)
6. C. Miao, M. Wang, Z. Yue, J. Zhou, Q. Li, Ceram. Int. **32**, 471 (2006)
7. S.F. Wang, Y.F. Hsu, Ceram. Int. **26**, 669 (2000)
8. R. Zuo, L. Li, Z. Gui, Mater. Sci. Eng. **326**, 202 (2002)
9. M. Kondo, M. Hida, K. Omote, O. Taniguchi, T. Mita, S. Umemiya, K. Kurihara, Sens. Actuators **109**, 143 (2003).
10. F. Chaput, J.P. Boilot et al., J. Am. Cer. Soc. **72**, 1355 (1989)
11. G.H. Haertling, C.E. Land, J. Am. Cer. Soc. **54**, 1 (1971)
12. J.S. Lee, M.S. Choi, N.V. Hung, Y.S. Kim, I.W. Kim, E.C. Park, S.J. Jeong, J.S. Song, Ceram. Int. (in press)
13. T. Hayashi, T. Hasegawa, J. Euro. Cer. Soc. **25**, 2437 (2005)
14. K.H. Chung, J.H. Yoo, C.B. Lee, D.C. Lee, Y.H. Jeong, H.G. Lee, Sens. Actuators **125**, 340 (2006)
15. B.M. Jin, I.W. Kim, J.S. Kim, D.S. Lee, C.W. Ahn, J.H. Kwon, J. S. Lee, J.S. Song, S.J. Jeong, J. Electroceramics **15**, 119 (2005)
16. W.D. Callister, Jr., *Materials Science and Engineering, An Introduction*, (Willey, New York, 2003), p. 620
17. JCPDS card No. 04-0783
18. JCPDS card No. 27-1199, 80-1351, 80-1352, 81-0861, 33-0784